ISSUE 28 MARCH 2023

GAṆANAM (गणनम्)

HIGH PERFORMANCE *COMPUTING* NEWSLETTER

INSTITUTE FOR PLASMA RESEARCH, INDIA

INSIDE THIS ISSUE
(3 Pages)

Coupling of Laser Energy to Cluster Electrons in Two Stages Without Any External Injection

Kalyani Swain (PhD Student, Basic Theory and Simulation Division, IPR)
Email: kalyani.swain@ipr.res.in

Charged particle acceleration (e.g.- electrons and ions) in laser-plasma interaction is an active research area due to its wide application in particle accelerators and table-top radiation sources (e.g. x-rays). Atomic clusters (a nanometric form of matter), as a unique target media, with locally high density (like solid targets) and globally low density (like gas targets), can produce energetic electrons, ions, and x-rays on effective coupling with an intense laser by absorbing more than 80% of laser energy [1]. Laser with intensity $I_0>10^{16}$ W/cm^2 and 780 − 800 nm wavelength (λ), laser absorption is mostly collision-less, and resonance absorption plays a vital role in this regime. For long duration laser pulse (>50 cycles), linear resonance (LR) takes place on sufficient coulomb explosion. However, for a few-cycle laser pulse (~10 fs or below), the absorption is due to anharmonic resonance (AHR). Various theoretical models, simulations, and experiments have reported the maximum energy absorption per cluster electron (E_A) in the non-relativistic intensity regime for a given set of laser-cluster parameters (particularly for laser intensity $I_0<10^{18}$ W/cm^2 and wavelength λ ~ 780 − 800 nm) and in most of the cases E_A is limited upto 3.17 times of ponderomotive energy (U_p) [2,3]. The question arises, can E_A be improved further?

An ambient magnetic field (B_{ext}~ 13-20 kilo Tesla) [4] in a transverse direction to laser polarization can enhance E_A up to 15-30 times at electron cyclotron resonance (ECR) Ω_{C0} = ω. In this study, we use a non-linear rigid sphere oscillator model (RSM) and an in-house developed three-dimensional electrostatic Particle-in-cell (3DESPIC) code [2] to study the energy absorption phenomena by cluster electrons. We take simulation box of size 1024^3 a.u., 64^3 a.u. grids with size Δx = Δy = Δz = 16 a.u. for timestep Δt = 0.1 a.u. To understand the dynamics of laser absorption by cluster electrons, we record the trajectory of 2176 PIC electrons at each Δt using *ANTYA* cluster at IPR. Figure 1 shows for a range of B_{ext} = 0 to 2ω, E_A is enhanced up to 30-70 U_p at intensity I_0 = 7.13 × 10^{16}W/cm^2. For this intensity, though E_A is greater in the case of PIC compared to RSM, at high-intensity (I_0=1.83×10^{17}W/cm^2), both show a quantitative agreement [5]. As relativistic mass increases, electrons quickly deviate from the standard non-relativistic ECR (figure 1, point B), but time-dependent relativistic-ECR (RECR) happens (figure 1, point C) with relativistic electron-cyclotron frequency ($\Omega_C = \Omega_{C0}/\gamma(t) = \omega$) which also contributes to enhanced E_A. For the low value of B_{ext} (figure 1, point A), absorption is mainly due to relativistic anharmonic frequency (Ω_{eff}), which occurs for the initial two cycles of the laser pulse, called 1st stage (figure 2, a1). As B_{ext} increases (point B in figure 1), γ of all electrons increase, and ECR (Ω_C) hits around 2.5 cycles of the laser pulse (figure 2, b1, red lines), leading to higher absorption called 2nd stage. For the peak value (point C in figure 1), due to the broad-band 5-fs (fwhm) laser pulse, ECR happens multiple times at central frequency (ω) as well as at side band frequencies (0.8ω and 1.2ω) which further enhances the absorption (figure 2, c1). Further numerically retrieving the phase difference (Δψ = |ψvₓ - ψEₓ|) between the laser electric field and the corresponding velocity component of each electron (in both PIC and RSM) using FFT, we find that AHR happens only for a short interval (less than half a laser period) where Δψ ≈ π (a necessary condition for maximum energy absorption). However, for the low value of B_{ext}, this short-lived condition quickly drops to initial π/2 (no absorption) without using the remaining field strength, which is still high enough to provide energy to the AHR-freed electron (figure 3, a1). In addition to the existing laser field, the ambient magnetic field (B_{ext}) at ECR (point B of figure 1) further energizes the AHR-freed electron in coupling with the remaining unused laser pulse. The required phase matching condition Δψ ≈ π is now maintained for a longer duration Δτ, leading to huge laser absorption up to E_A ≈ 36U_p (figure 3, b1). At the peak of the energy curve (point C of figure 1), Δψ is maintained even for a longer duration near π, and simultaneously maximum strength of the laser pulse enhances E_A up to 70 U_p (figure 3, c1). AHR first sets transverse momentum with which the liberated electron is self-injected into the remaining laser field, where B_{ext} re-orients its momentum and helps energize it further, enforcing improved phase-matching Δψ ≈ π as well as frequency matching for ECR/RECR. However, for ECR/RECR (second stage) to happen, a transverse momentum of the electron through AHR (first stage) is necessary. The PIC results are well supported by RSM.

> ***"An external magnetic field applied perpendicular to laser polarization (B_{ext}~13-20 kilo Tesla) can increase energy absorption per electron cluster by 36-70 U_p (15-30 times) at ECR Ω_C = ω."***

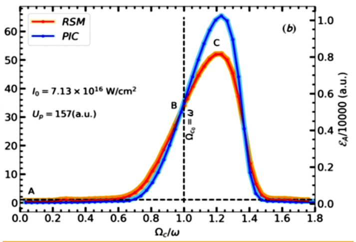

Figure 1: Comparison of RSM and PIC results: Average absorbed energy normalized with U_p($\mathcal{E}_A$= E_A/U_p :left axis) and in atomic units (right axis). Absorption at ECR (point B) is around 36U_p (0.15 MeV) and peaks at 65U_p~ 0.49 MeV (point C).

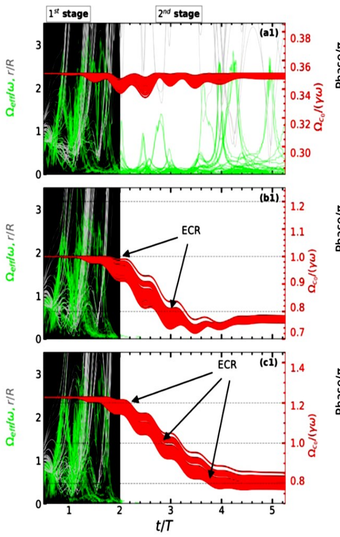

Figure 2: Time vs. frequency for PIC electrons, normalized Ω_{eff}/ω (green lines, left y-axis) and Ω_C/ω (red lines, right y-axis) for B_{ext} = 0.02, 0.057, 0.07 (a1, b1, c1) corresponds to point A, B, C of figure 1 respectively.

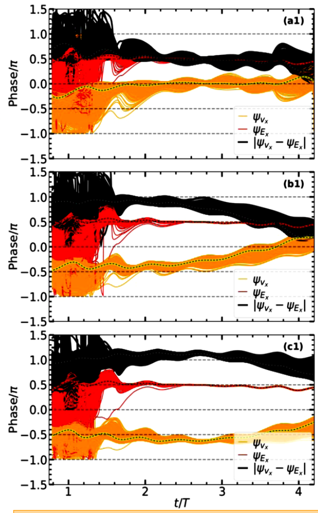

Figure 3: Phase analysis for PIC electrons. Phase angles ψvₓ , ψEₓ and Δψ of all PIC electrons for B_{ext} = 0.02, 0.057, 0.07 (a1, b1, c1) corresponds to point A, B, C of figure 1 respectively. Dashed lines indicates the respective average phase angles ∑vₓ/N and ∑Eₓ/N of all N electrons showing average system behavior.

References:

1. *T. Ditmire, E. Springate, et al., Phys. Rev. A 57, 369382 (1998).*
2. *M. Kundu and D. Bauer, Phys. Rev. Lett. 96, 123401 (2006).*
3. *S. S. Mahalik and M. Kundu, Physics of Plasmas 23, 123302 (2016).*
4. *M. Murakami, et al., "Generation of megatesla magnetic fields by intense-laser-driven microtube implosions," Scientific Reports 10, 16653 (2020).*
5. ***K. Swain**, S. S. Mahalik, and M. Kundu, Scientific Reports 12, 11256 (2022).*

Profiling Codes Using Intel VTune Profiler

This article focuses on how the Intel VTune Profiler can be used for profiling codes written in several programming languages. The performance statistics data collected from the profiler can enable users to identify and fix performance issues quickly, reducing development time and improving overall code performance and system efficiency. For more details, you may visit the intel website (click here)

What is Intel VTune Profiler?

Intel VTune Profiler (formerly known as VTune Amplifier till intel-2019) is a highly versatile and advanced profiling tool that provides comprehensive performance statistics for your code.

> *"Intel VTune Profiler can be used for profiling both serial and parallel codes."*

> *"Codes in Fortran, C, C++ can be profiled with Intel VTune Profiler."*

When to use Intel VTune Profiler?

It can help you to identify performance issues with the code and guide you in optimizing CPU usage and improving memory efficiency. If your code uses multithreading, it can enable you to analyze the performance of multiple threads as well.

How to Run on ANTYA?

Intel VTune Profiler is one of the tools included in the Intel HPC Toolkit. On ANTYA, there are several versions of Intel HPC toolkits, intel-2018, intel-2019 and intel-2020. After intel-2020, Intel Parallel Studio XE Cluster Edition transitioned into Intel oneAPI Toolkits and VTune is now part of oneAPI toolkits.

```
# Intel modules
[user@login1 ~]$ module avail intel-
intel-2018  intel-2019  intel-2020

# Availing Intel VTune Profiler (VTune Amplifier) from intel modules: The process from all the intel modules is the same. An example from intel-2019 is shown below:
[user@login1 ~]$ module load intel-vtune-2019
[user@login1 ~]$ amplxe-gui
# This will open a VTune GUI where you can set a project and launch a profile run.

# Availing Intel VTune Profiler (VTune Amplifier) from oneAPI:
[user@login1 ~]$ module load oneapi/modulefiles/vtune/2021.2.0
[user@login1 ~]$ vtune-gui
```

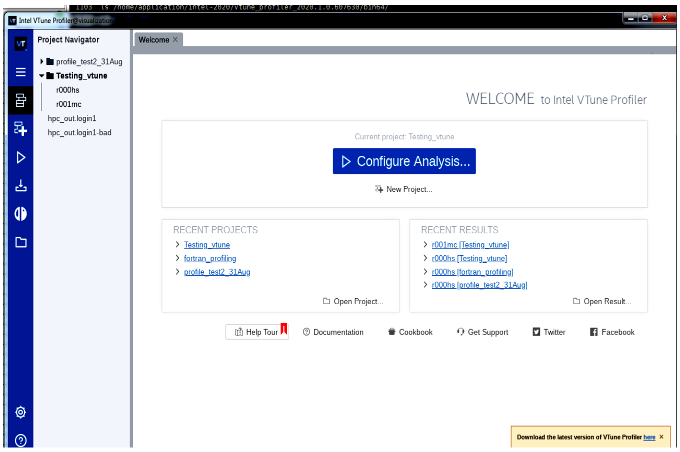

Create a new project. Choose the location of the project as your working directory

After setting up the project, provide the application which needs to be profiled.

Launch the run from the play button and wait for the analysis to finish

All the profiling runs need to be launched as an interactive job and should not be submitted on login nodes.

ANTYA UPDATES AND NEWS

1. New Packages/Applications Installed

⇒ New licensed MATLAB version available

module load MATLAB/2022b

This version with an academic license is meant for Educational and Research use only and runs from the visualization node.

HPC PICTURE OF THE MONTH

Crystallization in an Active-Passive Mixture

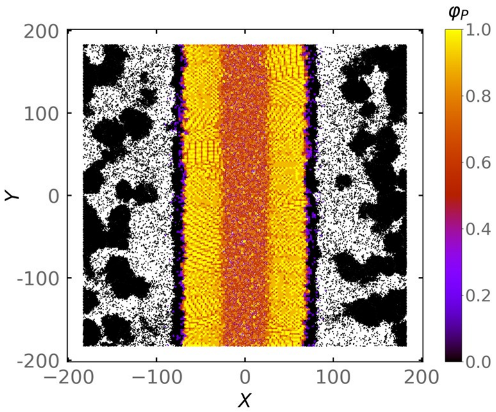

Pic Credit: **Anshika Chugh**

The figure shows density plots of local area fraction of passive particles at a steady time after a quench, starting with a fully segregated initial configuration with packing fraction 0.6. In areas where the local density approaches 1, we can observe indications of crystallization (yellow patches).

[Ref: Figure reproduced by Anshika Chugh, using IPR's MPMD2-A code based on parameters of Phys. Rev. Lett. 114, 018301]

The above figure has been created using data of 102400 particles that took 9 hours to generate using MPI **2-D MPMD-A code** on 40 cores of *ANTYA*.

TIP OF THE MONTH

Intel oneAPI and all its tools can be availed as modules now. For users using the intel modules, they may try to recompile their codes with oneAPI for better performance.

```
[user@login1 ~]$ module avail oneapi
# This will list all the modules available as part of oneAPI and based on requirement, anyone can be loaded.
```

ANTYA Utilization: FEBRUARY 2023

ANTYA Daily Observed Workload

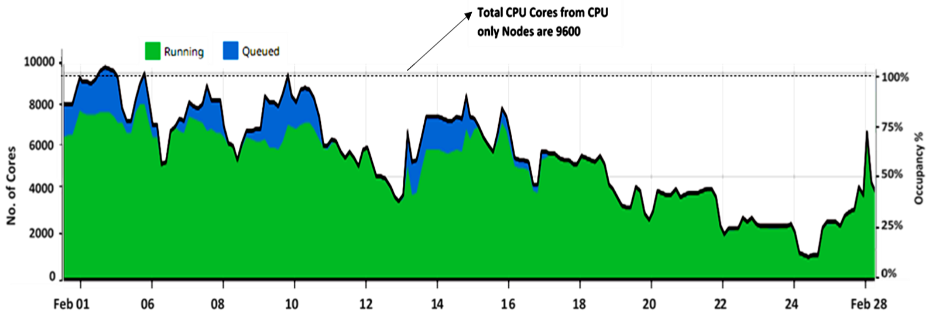

ANTYA HPC USERS' STATISTICS— FEBRUARY 2023

♦ **Total Successful Jobs — 1324**

♦ **Top Users** (Cumulative Resources):

- CPU Cores — Amit Singh
- GPU Cards — Shishir Biswas
- Walltime — Shishir Biswas
- Jobs — Someswar Dutta

Other Recent Work on HPC (Available in IPR Library)

The bifurcation behaviour of RMP control of ELMs in the presence of plasma flow : A nonlinear simulation study	Chandra Debasis
Study of E x B electron drift instability in Hall-thruster simulations using XOOPIC code	Sneha Gupta
Dynamics of electron Langmuir waves in the presence of inhomogeneous kinetic ions	Sanjeev Kumar Pandey
Ion-driven electron cloud dynamics in a non-axisymmetric torus: A 3D3V Particle-in-Cell study	Swapnali Khamaru
Plasma dynamics from application of edge biasing	Vijay Shankar
Nonlinear excitations within strongly coupled quasi-localized regime of dusty plasma	Prince Kumar
Vlasov simulations of whistler destabilization by electron beams having anisotropic velocity distribution	Gayatri Bhayyaji Barsagade
Poloidal gradient driven off-target circulation and upstream density shoulder in EMC3-Eirene simulations of inboard limited circular scrape off-layer plasma	Arzoo Malwal
Steep electrostatic excitations in highly quasi-longitudinal whistlers propagating along resonant cone.	Gayatri Bhayyaji Barsagade
Plasma Facing Component technologies and test facilities developments in India	Samir Sadashiv Khirwadkar
Effect of ion temperature on the dynamics of seeded impurities in the edge and SOL regions	Shrish Raj
Thermal fluctuations of Strongly Coupled Dusty Plasmas: A Theoretical and Experimental Study	Ankit Dhaka
Quest for magneto-convective unstable flow regime in horizontal MHD duct flows	Srikanta Sahu
Laser cluster interaction in external magnetic field: emergence of nearly mono-energetic weakly relativistic electron beam	Kalyani Swain
Collective behavior of self-propelled particles with a non-reciprocal reorientational interaction	Soumen De Karmakar
Whistler heat-flux instability governed interaction of anisotropic beam electrons in electromagnetic Vlasov simulations	Anjan Kumar Paul

Acknowledgement

The HPC Team, Computer Division IPR, would like to thank all Contributors for the current issue of *GAṆANAM*.

On Demand Online Tutorial Session on HPC Environment for New Users Available
Please send your request to ***hpcteam@ipr.res.in.***

Join the HPC Users Community
hpcusers@ipr.res.in
If you wish to contribute an article in GAṆANAM, please write to us.

Contact us
HPC Team
Computer Division, IPR
Email: ***hpcteam@ipr.res.in***